

# FAILURE MECHANISMS OF COMPOSITE SANDWICH STRUCTURES

E.E Gdoutos<sup>1</sup> and I.M. Daniel<sup>2</sup>

School of Engineering, Democritus University of Thrace, GR - 671 00 Xanthi, Greece  
Robert R. McCormick School of Engineering and Applied Science, Northwestern University, Evanston, IL 60208

## ABSTRACT

Sandwich construction is of particular interest and widely used, because the concept is very suitable and amenable to the development of lightweight structures with high in-plane and flexural stiffness. Sandwich panels consist typically of two thin face sheets (or facings, or skins) and a lightweight thicker core. They display various failure modes under general bending, shear and in-plane loading. The failure modes can be predicted by conducting a thorough stress analysis and applying appropriate failure criteria in the critical regions of the beams. The analysis is difficult because of the nonlinear and inelastic behavior of the constituent materials and the complex interactions of failure modes.

A thorough investigation of the failure mechanisms of composite sandwich beams under four- and three-point bending and cantilever beams was undertaken. The beams were made of unidirectional carbon/epoxy (AS4/3501-6) facings and a PVC closed-cell foam (Divinycell) core. Two types of core material H100 and H250 with densities 100 and 250 kg/m<sup>3</sup>, respectively, were used. The thickness of the facings and core were 1 mm and 25.4 mm, respectively.

The uniaxial tensile, compressive and shear stress-strain curves of the facings and core materials were obtained. It was found that unidirectional carbon/epoxy after an initial linear part exhibits a characteristic stiffening nonlinearity in tension and a softening nonlinearity in compression. The longitudinal strength in tension is about fifty percent higher than that in compression. The core material showed quite different stress-strain behavior in tension and compression. In compression the stress-strain curve shows a linear elastic – perfectly plastic behavior. At some point the load increases rapidly as the cells fully collapse and densification takes place. For the H100 core tensile strength along the longitudinal direction is eighty percent higher than the compressive strength, while for the H250 material the tensile strength is fifty percent higher. Both materials are anisotropic with the through-thickness tensile strength higher than the longitudinal tensile strength. The failure behavior of the core materials was modeled by the Tsai-Wu failure criterion.

Sandwich beams were loaded under bending moment and shear and failure modes were observed and compared with analytical predictions. The failure modes investigated are face sheet compressive failure, core failure and facing wrinkling. The various modes have been studied separately and both initiation and ultimate failure have been determined. Initiation of a particular failure mode and triggering and interaction with other failure modes was also investigated. A detailed stress and failure analysis was performed taking into account that a biaxial state of stress is developed in both the core and the facings. The stress state was combined with the Tsai-Wu failure criterion for both the core and the facings.

The initiation of the various failure modes depends on the material properties of the constituents (facings, adhesive, core), geometric dimensions and type of loading. The appropriate failure criteria should account for the complete state of stress at a point, including two- and three-dimensional effects. Failure modes were discussed according to the type of loading applied. In sandwich columns under compression, or beams in pure bending, compressive failure of the skins takes place if the core is sufficiently stiff in the through-the-thickness direction. Otherwise, facing wrinkling takes place. In the case of beams subjected to bending and shear the type of failure initiation depends on the relative magnitude of the shear component. When the shear component is low (long beams), facing wrinkling occurs first while the core is still in the linear elastic range. The critical stress at wrinkling can be predicted satisfactorily by an expression by Hoff and Mautner and depends only on the facing and core moduli. When the shear component is relatively high (e.g., short beams), core shear failure takes place first and is followed by compression facing wrinkling. Wrinkling failure follows but at a lower than predicted critical stress. The predictive expression must be adjusted to account for the reduced core moduli.

## 1. INTRODUCTION

Sandwich construction is of particular interest and widely used, because the concept is very suitable and amenable to the development of lightweight structures with high in-plane and flexural stiffness. Sandwich panels consist typically of two thin face sheets (or facings, or skins) and a lightweight thicker core. Commonly used materials for facings are composite laminates and metals, while cores are made of metallic and non-metallic honeycombs, cellular foams, balsa wood and trusses. The facings carry almost

all of the bending and in-plane loads and the core helps to stabilize the facings and defines the flexural stiffness and out-of-plane shear and compressive behavior.

The overall performance of sandwich structures depends on the material properties of the constituents (facings, adhesive and core), geometric dimensions and type of loading. Sandwich beams under general bending, shear and in-plane loading display various failure modes. Failure modes and their initiation can be predicted by conducting a thorough stress analysis and applying appropriate failure criteria in the critical regions of the beam including three-dimensional effects. This analysis is difficult because of the nonlinear and inelastic behavior of the constituent materials and the complex interactions of failure modes. For this reason, properly designed and carefully conducted experiments are important in elucidating the physical phenomena and helping the analysis.

Possible failure modes include tensile or compressive failure of the facings, debonding at the core/facing interface, indentation failure under concentrated loads, core failure, wrinkling of the compression face and global buckling. Following initiation of a particular failure mode, this mode may trigger and interact with other modes and final failure may follow another failure path. A substantial amount of work has been reported on failure of sandwich panels [1-4]. Recently, the authors and coworkers have performed a thorough investigation of the failure behavior of sandwich beams with facings made of carbon/epoxy composite material [5-15]. The various modes have been studied separately and both initiation and ultimate failure have been determined.

In the present work, failure modes were investigated experimentally in axially loaded composite sandwich columns, sandwich beams under four-point and three-point bending and end-loaded cantilever beams. Failure modes observed and studied include face sheet compressive failure, face sheet debonding, indentation failure, core failure and face sheet wrinkling.

## 2. CHARACTERIZATION OF CONSTITUENT MATERIALS

The sandwich beam facings were unidirectional carbon/epoxy plates (AS4/3501-6), fabricated separately by autoclave molding. Uniaxial tensile and compressive tests were conducted primarily in the longitudinal direction in order to obtain the relevant constitutive behavior of the facing material. The compressive tests were performed using a new fixture developed at Northwestern University [16]. The concept of the fixture is to transmit the initial part of the load through the tabs by shear loading and thereafter engage the ends to apply the additional load to failure by end loading. The longitudinal tensile and compressive stress-strain behavior for the AS4/3501-6 carbon/epoxy is shown in Fig. 1, where it is seen that the material exhibits a characteristic stiffening nonlinearity in tension and softening nonlinearity in compression.

Three core materials were investigated. One of them was aluminum honeycomb (PAMG 8.1-3/16 001-P-5052, Plascore Co.). The other core materials investigated were two types of PVC closed-cell foam, Divinycell H100 and H250, with densities of 100 and 250 kg/m<sup>3</sup>, respectively. The aluminum honeycomb material is highly anisotropic with much higher stiffness and strength in the through-the-thickness direction (cell direction) than in the in-plane directions. The three principal moduli  $E_1$ ,  $E_2$  and  $E_3$  (along the cell axis) were obtained by means of four-point bending, three-point bending and pure compression tests [17]. The span length of the bending specimens was 20.3 cm. The distance between the loads in the four-point bending tests was 10.2 cm. The specimens had a cross section of 2.54 x 2.54 cm. The out-of-plane shear modulus  $G_{13}$  was obtained by means of a rail shear test. The lower density foam core material, Divinycell H100, exhibits nearly isotropic behavior. The higher density foam, Divinycell H250, exhibits pronounced axisymmetric anisotropy with much higher stiffness and strength in the cell direction (3-direction).

To determine the in-plane stress-strain behavior of the materials in compression, prismatic specimens of dimensions 25.4 x 25.4 x 76.2 mm were tested quasi-statically in an Instron servo-hydraulic testing system. Both longitudinal and transverse strains were measured with extensometers. The longitudinal strains were monitored on opposite sides of the specimen to insure that there was no bending effect during loading. The tests were terminated after the load dropped and remained almost constant following a peak value.

For the through-the-thickness stress-strain behavior of the materials in compression, specimens of the same dimensions as for the in-plane direction were used. The specimens were made by bonding together three cubes of the material of 25.4 mm side along the thickness direction. The cubes were bonded using a commercially available epoxy adhesive (Hysol EA 9430). The specimens used for tension tests along the in-plane direction had dimensions 6.4 x 25 x 200 mm. The specimens were tabbed with 100 mm long glass/epoxy tabs which were bonded over a length of 50 mm at the specimen ends with epoxy adhesive

(Hysol 907). The space between the extended parts of the tabs was filled in with high modulus epoxy filler (Hysol EA 9430).

For the tension tests in the through-the-thickness direction, prismatic specimens of dimensions 13 x 25 x 200 mm were made by assembling and bonding together fifteen triangular prismatic pieces of the material. The specimens were tabbed with glass/epoxy tabs as described before for the in-plane tension tests. Both types of specimens were gripped over the extended and filled portion of the tabs to avoid crushing of the foam. They were loaded quasi-statically to failure in a servo-hydraulic testing machine (Instron). Strains were measured with an extensometer attached to the specimen.

Fig. 2 shows stress-strain curves for this material under uniaxial tension and compression along the in-plane (1) and through-the-thickness (3) directions. The material displays different behavior in tension and compression with tensile strengths much higher than corresponding compressive strengths. The uniaxial stress-strain behavior in tension is nonlinear elastic without any identifiable yield region. In uniaxial compression the material is nearly elastic-perfectly plastic in the initial stage of yielding.

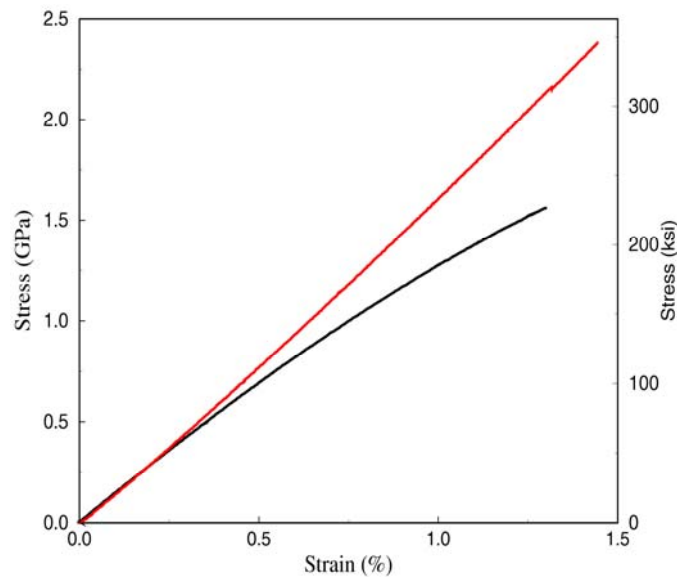


Figure 1: Stress-strain curves in tension (exhibiting hardening nonlinearity) and compression (exhibiting softening nonlinearity) of carbon/epoxy facings (AS4/3501-6)

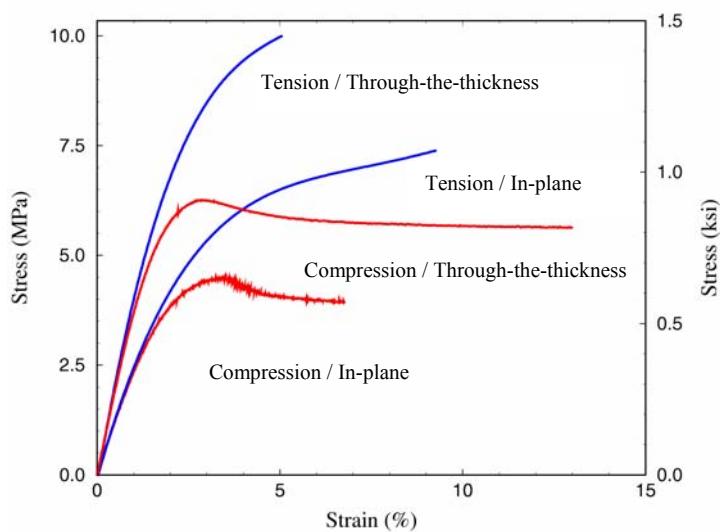


Figure 2: Stress-strain curves of PVC foam (Divinycell H250).

The shear stress-strain behavior on the 1-3 plane was determined by the Arcan test and is shown in Fig. 3. The shear behavior is also nearly elastic - perfectly plastic. Some characteristic properties of the sandwich constituent materials investigated are tabulated in Table 1.

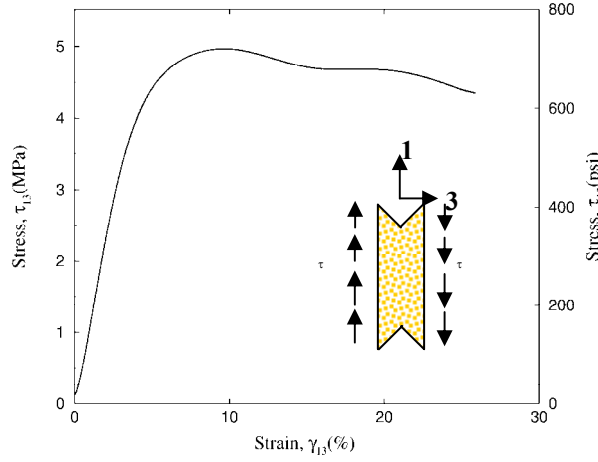


Figure 3: Shear stress-strain curve of PVC foam (Divinycell H250)

A common failure mode in sandwich construction is the so-called "core shear failure," in which the core fails when the shear stress reaches its critical value. However, although the shear stress is usually the dominant one in the core, there are situations in which the normal stresses in the core are of comparable magnitude or even higher than the shear stresses. Under such circumstances a material element in the core may be subjected to a multi-axial state of stress. Therefore, proper design of sandwich structures requires failure characterization of the core material under combined stresses.

The higher density foam (Divinycell H250) core was fully characterized under multiaxial states of stress in the 1-3 plane [18]. A number of tests were conducted to define a failure surface for the material. Experimental results conformed well with the Tsai-Wu failure criterion for anisotropic materials as shown in Fig. 4. The Tsai-Wu criterion for a general two-dimensional state of stress on the 1-3 plane is expressed as follows

$$f_1 \sigma_1 + f_3 \sigma_3 + f_{11} \sigma_1^2 + f_{33} \sigma_3^2 + 2f_{13} \sigma_1 \sigma_3 + f_{55} \tau_5^2 = 1 \quad (1)$$

where

$$f_1 = \frac{1}{F_{1t}} - \frac{1}{F_{1c}}, \quad f_3 = \frac{1}{F_{3t}} - \frac{1}{F_{3c}}$$

$$f_{11} = \frac{1}{F_{1t} F_{1c}}, \quad f_{33} = \frac{1}{F_{3t} F_{3c}}, \quad f_{13} = -\frac{1}{2} (f_{11} f_{33})^{1/2}, \quad f_{55} = \frac{1}{F_5^2}$$

$F_{1t}, F_{1c}, F_{3t}, F_{3c}$  = tensile and compressive strengths in the in-plane (1, 2) and out-of-plane (3) directions

$F_5$  = shear strength on the 1-3 plane

Setting  $\tau_5 = k F_5$ , Eq. (1) is rewritten as

$$f_1 \sigma_1 + f_3 \sigma_3 + f_{11} \sigma_1^2 + f_{33} \sigma_3^2 + 2f_{13} \sigma_1 \sigma_3 = 1 - k^2 \quad (2)$$

The failure surface described by the Tsai-Wu criterion is an ellipsoid in the  $\sigma_1, \sigma_3, \tau_{13}(\tau_5)$  space displaced toward the tension-tension quadrant. It is seen that the material can sustain shear stresses  $\tau_{13}(\tau_5)$  up to 17% higher than the pure shear strength ( $F_5$ ). The most critical region for the material is the compression-compression quadrant. The most critical combination is compression and shear.

Table 1: Properties of constituent materials

	Facing	Honeycomb Core	FM-73 Adhesive	Foam Core (H100)	Foam Core (H250)
Density, $\rho$ , kg/m <sup>3</sup>	1,620	129	1,180	100	250
Thickness, h, mm	1.01	25.4	0.05	25.4	25.4
Longitudinal Modulus, $E_1$ , MPa	147,000	8.3	1,700	120	228
Transverse Modulus, $E_3$ , MPa	10,350	2,415		139	403
Transverse Shear Modulus, $G_{13}$ , MPa	7,600	580	110	48	117
Longitudinal Compressive Strength, $F_{1c}$ , MPa	1,930	0.2		1.7	4.5
Transverse Compressive Strength, $F_{3c}$ , MPa	240	11.8		1.9	6.3
Transverse Shear Strength, $F_{13}$ , MPa	71	3.5	33	1.6	5.0

### 3. EXPERIMENTAL PROCEDURE

The honeycomb core was 2.54 cm wide and was machined from a 2.54 cm thick sheet along the stiffer in-plane direction. The 2.54 cm wide composite facings were machined from unidirectional plates, bonded to the top and bottom faces of the honeycomb core with FM73 M film adhesive and the assembly was cured under pressure in an oven following the recommended curing cycle for the adhesive. Sandwich beams were also prepared by bonding composite facings to foam cores of 2.54 x 2.54 cm cross section using an epoxy adhesive (Hysol EA 9430) [17]. The adhesive was cured at room temperature by subjecting the sandwich beam to vacuum. The cured adhesive layer was 0.13 mm thick.

Special fixtures were fabricated for beams subjected to three-point and four-point bending and for end-loaded cantilever beams. In studying the effects of pure bending special reinforcement was provided for the core at the outer sections of the beam to prevent premature core failures. Also, under three-point bending, the faces directly under concentrated loads were reinforced with additional layers of carbon/epoxy to suppress and prevent indentation failure. Only in the case when the indentation failure mode was studied there was no face reinforcement.

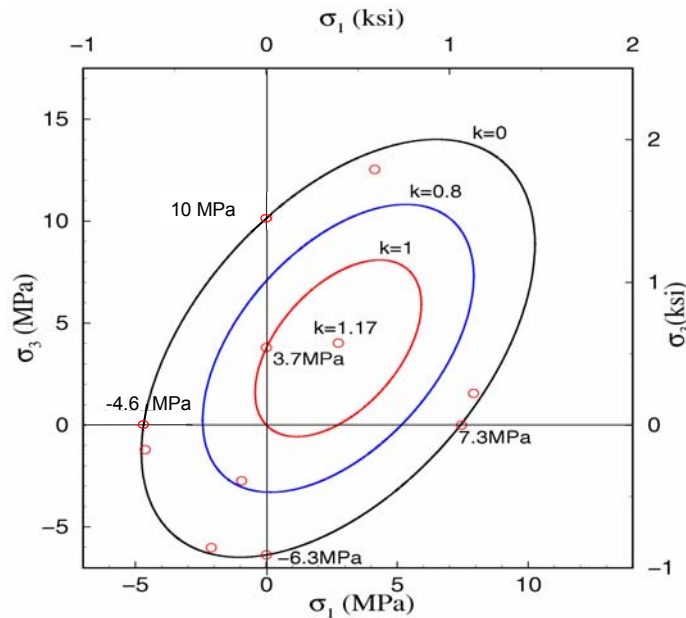


Figure 4: Failure envelopes predicted by the Tsai-Wu failure criterion for PVC foam (Divinycell H250) for  $k = 0, 0.8$  and  $1$ , and Experimental results ( $k = \tau_{13}/F_{13} = \tau_5/F_5$ )

Strains on the outer and inner (interface between facing and core) surfaces of the facings were recorded with strain gages. Beam deflections were measured with a displacement transducer (LVDT) and by monitoring the crosshead motion. The deflection was also monitored with a coarse moiré grating (31 lines/cm). Longitudinal and transverse strains in the core were measured with finer moiré gratings of 118 lines/cm and 200 lines/cm.

The deformation of the core was also monitored with birefringent coatings using reflection photoelasticity. Coatings, 0.5 mm and 1 mm thick, were used (PS-4D coatings, Measurements Group). The coating is bonded to the surface of the core with a reflective cement to insure light reflection at the interface. A still camera and a digital camcorder were used to record moiré and isochromatic fringe patterns. The fringe order of this pattern is related to the difference of principal strains as follows:

$$\varepsilon_1^c - \varepsilon_3^c = \varepsilon_1^s - \varepsilon_3^s = \frac{N\lambda}{2hK} \quad (3)$$

where  $N$  is the fringe order,  $\lambda$  is the wavelength of the illuminating light,  $h$  is the coating thickness and  $K$  is a calibration constant for the coating material. Superscripts  $s$  and  $c$  denote specimen and coating, respectively. The reinforcement effect of the birefringent coatings was neglected.

#### 4. FAILURE MODES

##### Sandwich Columns under Axial Compression

Possible failure modes in a sandwich column under axial compression include facing compressive failure, facing wrinkling, global buckling and core shear instability. Core compressive failure is unlikely because of its low stiffness and high ultimate (yield) strain. Because of the much higher stiffness of the facing material, the axial compressive stress in the facing is given by

$$\sigma_f \cong \frac{P}{2bh_f} \quad (4)$$

where  $P$  = applied load,  $h_f$  = facing thickness, and  $b$  = width of column cross section.

Facing compressive failure occurs when

$$\sigma_f = \frac{P}{2bh_f} = F_{1c} \quad (5)$$

where  $F_{1c}$  = compressive strength of facing material (here the longitudinal compressive strength of the composite).

Face wrinkling occurs when the facing stress reaches a critical value. One expression given by Heath and modified here is [19]:

$$\sigma_{cr} = \left[ \frac{2}{3} \frac{h_f}{h_c} \frac{E_{c3} E_{f1}}{(1 - \nu_{13} \nu_{31})} \right]^{1/2} \quad (6)$$

where  $h_c$  = core thickness,  $E_{f1}$  = longitudinal modulus of the face,  $E_{c3}$  = through-the-thickness modulus of the core,  $\nu_{ij}$  ( $i, j = 1, 3$ ) = Poisson's ratios of facing material associated with loading in the  $i$ -direction and deformation in the  $j$ -direction.

Three sandwich columns with three core materials, aluminum honeycomb, Divinycell H100 and Divinycell H250, were tested in compression. The sandwich columns had a height of 76.2 mm and a cross-sectional area of 25.4 x 25.4 mm. The facing stresses at failure were measured and compared with predicted critical values by Eqs. (5) or (6). Fig. 5 shows failure patterns of two columns with Divinycell H250 (Fig. 6a) and Divinycell H100 (Fig. 6b) foam cores. In the case of the honeycomb core, the measured failure stress indicates compressive facing failure according to Eq. (5). This behavior is explained from the high-out-of-plane stiffness of the honeycomb core, which results in a critical wrinkling stress predicted by Eq. (6) higher than the compressive strength of the facing. In the case of

foam cores failure occurred by facing wrinkling as predicted by Eq. (6). The measured values were somewhat lower than predicted due to material imperfections.

Global buckling depends on end conditions and material properties in a more complex manner as discussed by Vinson [20]. Core shear instability depends primarily on the shear modulus of the core and the core and facing thickness [20]. Neither one of these two modes was observed in the tests conducted.

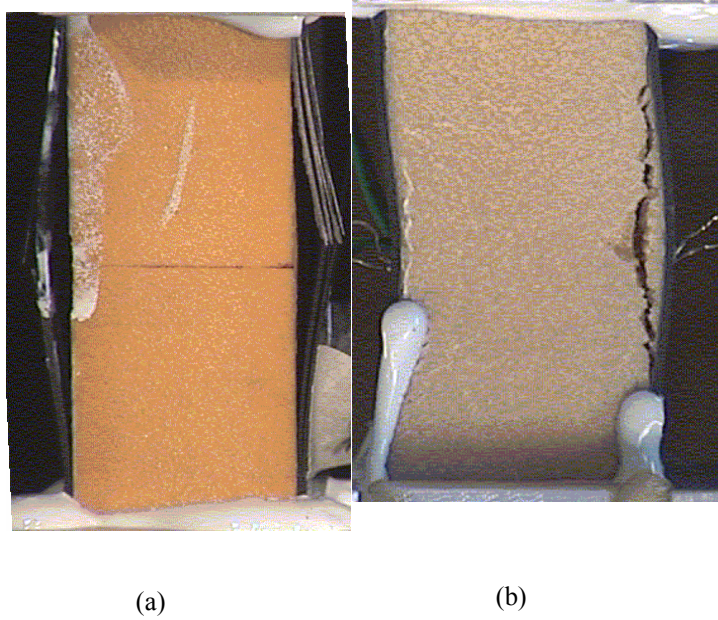


Figure 5: Failure of sandwich columns (a) Divinycell H250 core, (b) Divinycell H100 core

#### Sandwich Beams under Pure Bending

Under pure bending (or four-point bending) the moment is primarily carried by the much stiffer facings. For relatively thin facings and relatively low core stiffness, the facing stress is

$$\sigma_f \cong \frac{M}{bh_f(h_f + h_c)} \quad (7)$$

where  $M$  = applied moment, and  $b$  = beam width.  
Compressive failure occurs in the facing when

$$\sigma_f \cong \frac{M}{bh_f(h_f + h_c)} = F_{fc} \quad (8)$$

where  $F_{fc}$  = compressive strength of facing material. This mode of failure occurs in beams with cores of sufficiently high stiffness in the core direction, such as aluminum honeycomb. Fig. 6 shows experimental and predicted moment-strain curves for facings of a beam under four-point bending where the failure mode was compressive failure of the skin as predicted by Eq. (8).

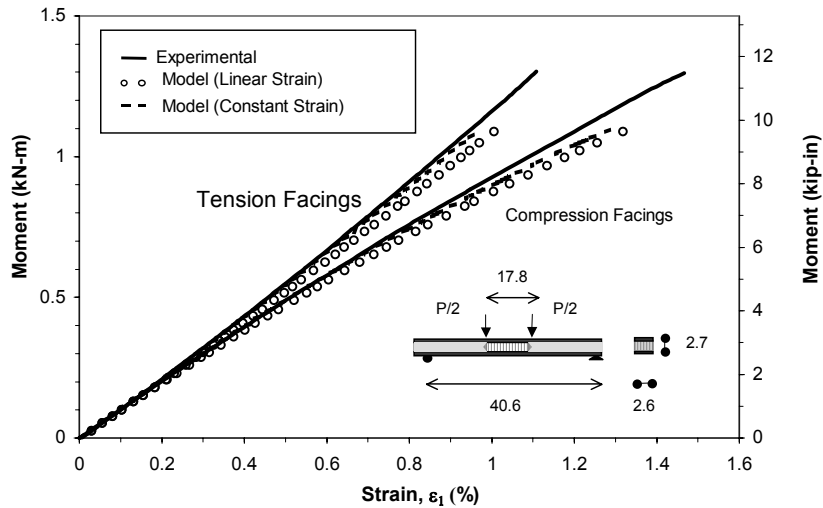


Figure 6: Experimental and predicted moment-strain curves for two facings of composite sandwich beam under four-point bending (dimensions are in cm)

For lower stiffness cores, a more likely failure mode is facing wrinkling as predicted by the modified Heath expression, Eq. (6). Facing wrinkling failure will occur when the predicted critical stress by Eq. (6) is less than the compressive strength of the facing material. The value of core modulus at transition from skin wrinkling to facing compressive failure is obtained from Eqs (6) and (8) as

$$E_{c3} = \frac{3}{2} \frac{h_c}{h_f} \frac{1 - \nu_{13} \nu_{31}}{E_{f1}} F_{fc}^2 \quad (9)$$

For values of the core modulus greater than calculated by Eq. (9), failure is governed by the compressive strength of the facing material. For core moduli lower than calculated above, facing wrinkling failure takes place and is controlled by the core modulus.

Fig. 7 shows moment-strain curves for two beams with Divinycell H100 foam cores under four-point bending. Failure in both cases is due to facing wrinkling. The measured facing stress at failure is relatively close to the predicted critical wrinkling stress by Heath's formula, Eq. (6).

Measured:  $\sigma_{cr} = 670$  MPa

Predicted:  $\sigma_{cr} = 715$  MPa

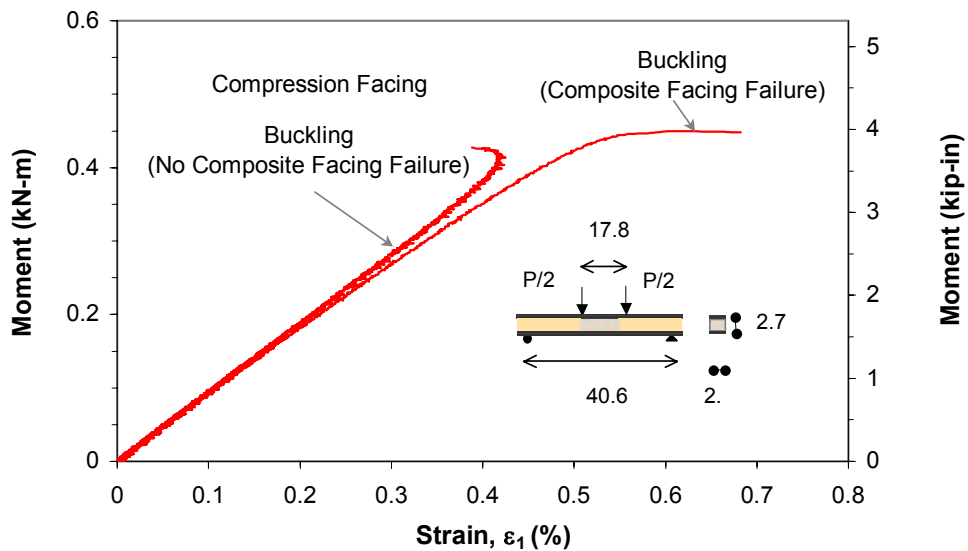


Figure 7: Facing wrinkling in sandwich beam under four-point bending (Divinycell H100 foam core, dimensions are in cm)



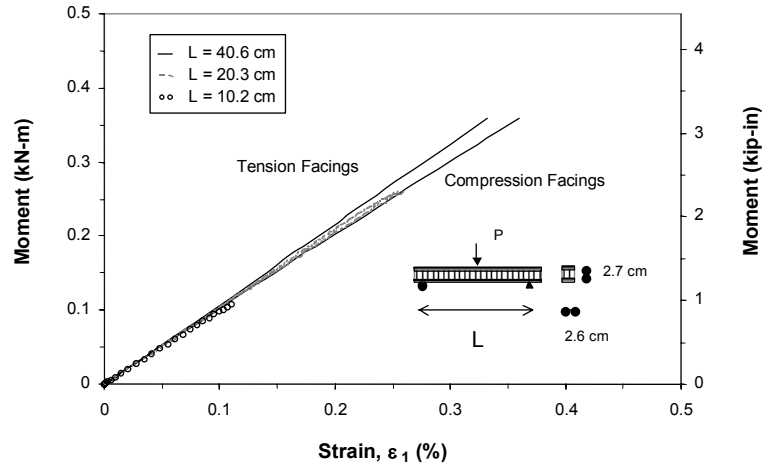


Figure 8: Applied moment versus maximum facing strain for beams of different span length under three-point bending

### Sandwich Beams under Bending and Shear

Beams under three-point bending and end-loaded cantilever beams are subjected to both bending moment and shear. It is assumed that the core and facings in the vicinity of the applied load are locally reinforced to suppress any possible indentation failure. The latter is the subject of another study [5, 9, 21]. The bending moment is primarily carried by the facings and the shear by the core. Excluding indentation, possible failure modes include core shear failure, core failure under combined shear and compression, facing wrinkling and facing compressive failure.

Sandwich beams with aluminum honeycomb cores under three-point bending failed due to early shear crimping of the core. The shear force at failure remained nearly constant for varying span lengths. This means that as the span length increases, the applied maximum moment and, thereby, the maximum face sheet strains at failure increase (Fig. 8). The results also indicate that the bending moment is carried almost entirely by the face sheets. The average shear stress at failure from the three tests represented in Fig. 8 is  $\tau^u = 3.59 \text{ MPa}$  which compares well with the measured shear strength of the honeycomb material of  $F_c = 3.59 \text{ MPa}$

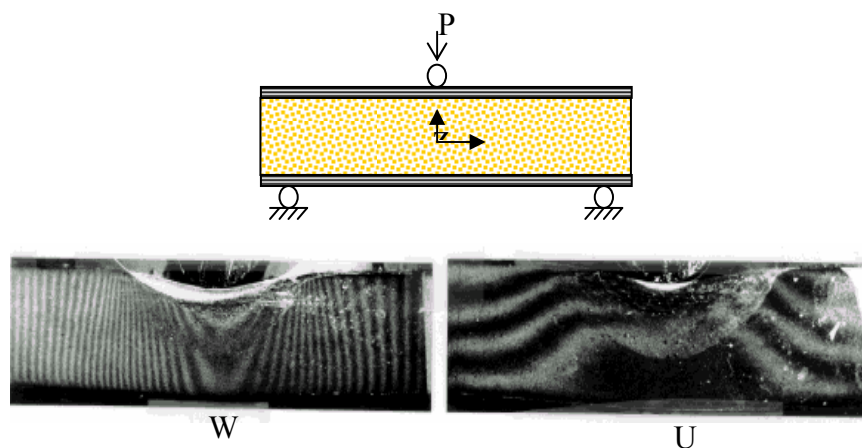


Figure 9: Moiré fringe patterns corresponding to horizontal and vertical displacements in sandwich beam under three-point bending (12 lines/mm, Divinycell H250 core)

The deformation and failure mechanisms in the core were studied experimentally by means of moiré gratings and birefringent coatings. Fig. 9 shows moiré fringe patterns for the vertical,  $w$ , and horizontal,  $u$ , displacements in the core of a sandwich beam with Divinycell H250 foam core under three-point bending. They were obtained with specimen gratings of 11.8 lines/mm and a master grating of the same pitch with lines parallel to the longitudinal and vertical directions. The moiré fringe patterns of Fig. 9 corresponding to the horizontal ( $u$ ) displacements away from the applied load consist of nearly parallel and equidistant fringes from which it follows that

$$\varepsilon_x = \frac{\partial u}{\partial x} \cong 0, \quad \frac{\partial u}{\partial z} \cong C_1 \quad (10)$$

where  $C_1$  is a constant.

Similarly, the moiré fringe patterns corresponding to the vertical ( $w$ ) displacements away from the applied load consist of nearly parallel and equidistant fringes from which it follows that

$$\varepsilon_z = \frac{\partial w}{\partial z} \cong 0, \quad \frac{\partial w}{\partial x} \cong C_2 \quad (11)$$

where  $C_2$  is constant.

From Eqs (10) and (11) it follows that

$$\gamma_{xz} = \frac{\partial u}{\partial z} + \frac{\partial w}{\partial x} \cong \text{constant} \quad (12)$$

Eq. (12) indicates that the core is under nearly uniform shear strain, and therefore, under nearly uniform shear stress. Furthermore, Eqs (10) and (11) indicate that the normal strains  $\varepsilon_x$  and  $\varepsilon_z$  in the core are nearly zero or very small compared to the shear strain. This is in accordance with the classical bending theory of sandwich beams. The bending moment is taken mainly by the tensile and compressive facings. This results in high facing normal stresses with low normal strains due to the high Young's modulus of the facings. On the other hand the shearing force is taken mainly by the core, resulting in high core strains due to the low shear modulus of the core. Thus, the core is under nearly uniform shear stress. This is true only in the linear range as shown by the isochromatic fringe patterns of the birefringent coating in Fig. 10. In the nonlinear and plastic region the core begins to yield and the shear strain becomes highly nonuniform peaking at the center. From fringe patterns like those of Fig. 10 it was found that the shear deformation starts becoming nonuniform at an applied load of 3.29 kN which corresponds to an average shear stress of 2.55 MPa. This is close to the proportional limit of the shear stress-strain curve of Fig. 3. As the load increases the shear strain in the core becomes nonuniform peaking at the center is illustrated in Fig. 4.

Core failure is accelerated when compressive and shear stresses are combined. This critical combination is evident from the failure envelope of Fig. 4. The criticality of the compression/shear stress biaxiality was tested with a cantilever sandwich beam loaded at the free end. The cantilever beam was 25.4 cm long. A special fixture was prepared to provide the end support of the beam. The isochromatic fringe patterns of the birefringent coating in Fig. 10 show how the peak birefringence moves towards the fixed end of the beam at the bottom where the compressive strain is the highest and superimposed on the shear strain.

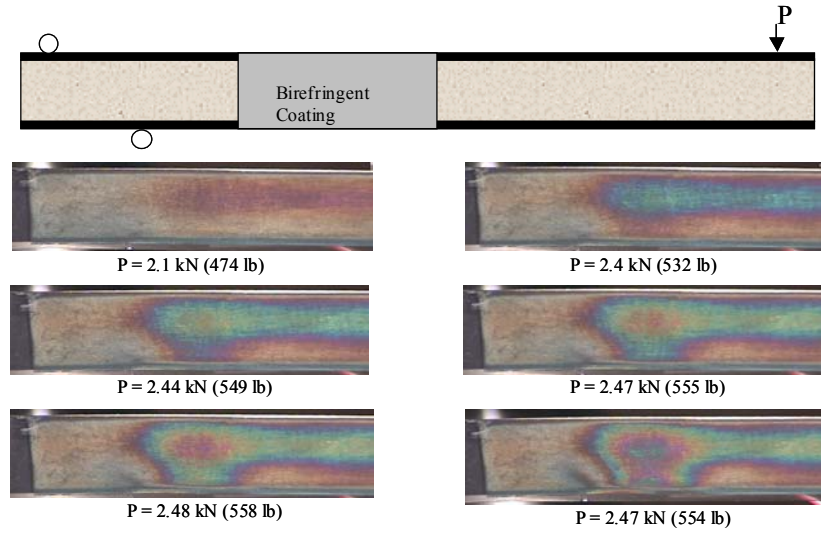


Figure 10: Isochromatic fringe patterns in birefringent coating of a cantilever sandwich beam under end load

Plastic deformation of the core, whether due to shear alone or a combination of compression and shear, degrade the supporting role of the core and precipitate other more catastrophic failure modes, such as facing wrinkling.

In the present case of beams subjected to bending and shear, compression facing wrinkling is influenced by the shear as well as the axial stiffnesses of the core in the through-the-thickness direction. A prediction of the critical facing wrinkling stress for this case was given by Hoff and Mautner [22].

$$\sigma_{cr} = c(E_{f1} E_{c3} G_{cl3})^{1/3} \quad (13)$$

where  $c$  is a constant usually taken equal to 0.5. In this relation the core moduli are the initial elastic moduli if wrinkling occurs while the core is still in the linear elastic range. This requires that the shear force at the time of wrinkling be low enough or, at least,

$$V < A_c F_{cs} \quad (14)$$

where  $A_c$  = core cross sectional area  
 $F_{cs}$  = core shear strength

Sandwich beams with Divinycell H250 foam cores were tested under three-point bending and as cantilever beams, while monitoring strain on the face sheets, at points of highest compressive stress. Moment-strain curves for three such beams are shown in Fig. 11. The maximum moment recorded is an indication of facing wrinkling. For the cantilever beam and one of the beams loaded in three-point bending, the facing wrinkling obtained from the experiments are:

$$\sigma_{cr} = 910 \text{ MPa} \quad (\text{cantilever})$$

$$\sigma_{cr} = 715 \text{ MPa} \quad (\text{three-point bending})$$

The calculated value from eq. (11) is

$$\sigma_{cr} = 945 \text{ MPa}$$

In the case of the short beam the experimental critical stress at facing wrinkling is  $\sigma_{cr}=500$  MPa.

This lower than predicted value is attributed to the fact that the shear loading component is significant and core failure precedes facing wrinkling. Core failure takes the form of core yielding, which results in reduced Young's modulus. This reduces the core support of the facing and precipitates facing wrinkling at a lower stress. The critical wrinkling stress in this case could be predicted by a modification of expression (13) as

$$\sigma_{cr} = 0.5 (E_{f1} E'_{c3} G'_{cl3})^{1/3} \quad (15)$$

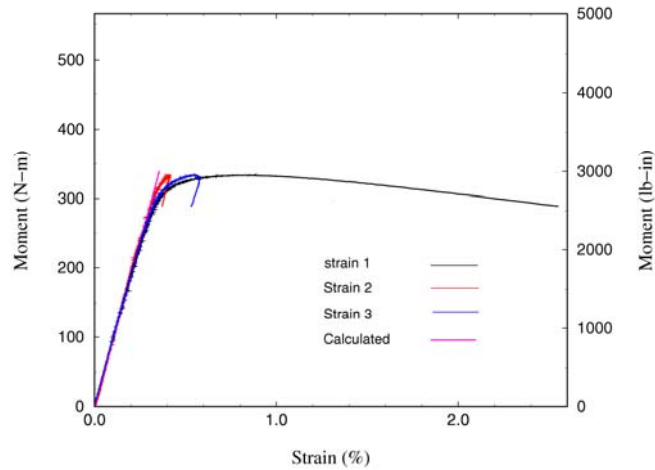


Figure 11: Moment-strain curves for beams in three-point bending

where  $E'_{c3}$  and  $G'_{c13}$  are the reduced core moduli. The determination of these moduli would require an exact elastic-plastic stress analysis of the beam.

It is obvious from the above that failure modes, their initiation, sequence and interaction depend on loading conditions. In the case of beams under three-point bending this is illustrated by varying the span length. For short spans, core failure occurs first and then it triggers facing wrinkling. For long spans, facing wrinkling can occur before any core failure. Core failure initiation can be described by calculating the state of stress in the core and applying the Tsai-Wu failure criterion. This yields a curve for critical load (at core failure initiation) versus span length. On the other hand, in the absence of core failure, facing wrinkling can be predicted by Eq. (11) and expressed in terms of a critical load as a function of span length. Fig. 12 shows curves of the critical load versus span length for initiation of the two failure modes discussed above. Their intersection defines the transition from core failure initiation to facing wrinkling initiation. For a beam with carbon/epoxy facings (8-ply unidirectional AS4/3501) and PVC foam core (Divinycell H250) of  $2.5 \times 2.5$  cm cross section, the span length for failure mode transition is  $L = 35$  cm.

Although the results above are at least qualitatively explained by available theory, it is apparent that better theoretical modeling is needed. The theoretical prediction of facing wrinkling, Eq. (13), gives equal weight to the three moduli involved and is independent of facing and core dimensions. A more sound theory should take into consideration the nonlinear and inelastic biaxial stress-strain behavior of the core material and the stress/strain redistribution following core yielding.

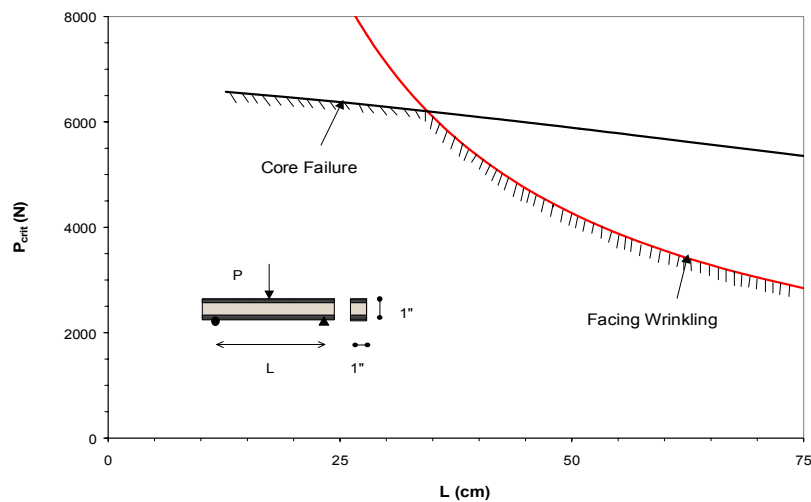


Figure 12: Critical load versus span length for initiation of core failure and facing wrinkling.

## 5. CONCLUSIONS

The initiation of the various failure modes in composite sandwich beams depends on the material properties of the constituents (facings, adhesive, core), geometric dimensions and type of loading. The appropriate failure criteria should account for the complete state of stress at a point, including two- and three-dimensional effects. Failure modes were discussed according to the type of loading applied.

In sandwich columns under compression, or beams in pure bending, compressive failure of the skins takes place if the core is sufficiently stiff in the through-the-thickness direction. Otherwise, facing wrinkling takes place, which can be predicted by Heath's formula. Experimental results were close to predicted ones.

In the case of beams subjected to bending and shear the type of failure initiation depends on the relative magnitude of the shear component. When the shear component is low (long beams), facing wrinkling occurs first while the core is still in the linear elastic range. The critical stress at wrinkling can be predicted satisfactorily by an expression by Hoff and Mautner and depends only on the facing and core moduli. When the shear component is relatively high (e.g., short beams), core shear failure takes place first and is followed by compression facing wrinkling. Wrinkling failure follows but at a lower than predicted critical stress. The predictive expression must be adjusted to account for the reduced core moduli.

## REFERENCES

1. Allen, H. G., *Analysis and Design of Structural Sandwich Panels*, Pergamon Press, London, (1969).
2. Hall, D. J. and Robson, B. L., A Review of the Design and Materials Evaluation Programme for the GRP/Foam Sandwich Composite Hull of the RAN Minehunter, *Composites*, Vol.15, pp 266-276, 1984.
3. Zenkert, D., *An Introduction to Sandwich Construction*, Chameleon, London, (1995).
4. Daniel, I. M., Gdoutos, E. E., Wang, K.-A. and Abot, J. L., 2001, Failure Modes of Composite Sandwich Beams, *International Journal of Damage Mechanics*, Vol. 11, pp. 309-334, 2002.
5. Gdoutos, E.E., Daniel I.M., and Wang, K.-A., Indentation Failure of Sandwich Panels," *Proceedings of the 6th Greek National Congress on Mechanics*, edited by E.C. Aifantis and A.N. Kounadis, July 19-21, 2001, Thessaloniki, Greece, pp. 320-326, 2001.
6. Daniel, I.M., Gdoutos, E.E and Wang, K.-A., Failure of Composite Sandwich Beams, *Proceedings of the Second Greek National Conference on Composite Materials, HELLAS-COMP 2001*, Patras, Greece, 6-9 June 2001, 2001.
7. Daniel, I.M., Gdoutos, E.E., Abot, J.L. and Wang, K.-A., Core Failure Modes in Composite Sandwich Beams, *ASME International Mechanical Engineering Congress and Exposition*, New York, November 11-16, 2001, in *Contemporary Research in Engineering Mechanics*, edited by G.A. Kardomateas and V. Birman, AD-Vol. 65, AMD-Vol. 249, pp. 293-303, 2001.
8. Gdoutos, E.E., Daniel, I.M., Abot, J.L and Wang, K.-A., Effect of Loading Conditions on Deformation and Failure of Composite Sandwich Structures, *Proceedings of ASME International Mechanical Engineering Congress and Exposition*, New York, November 11 -16, 2001.
9. Gdoutos, E.E., Daniel, I.M. and Wang, K.-A., Indentation Failure in Composite Sandwich Structures, *Experimental Mechanics*, Vol.42, pp.426-431, 2002.
10. Daniel, I.M., Gdoutos, E.E and Wang, K.-A., Failure of Composite Sandwich Beams, *Advanced Composites Letters*, Vol.11, pp. 49-57, 2002.
11. Abot, J.L., Daniel, I.M., and Gdoutos, E.E. Failure Mechanisms of Composite Sandwich Beams Under Impact Loading, *Proceedings of the 14th European Conference on Fracture*, Cracow, September 8-13, 2002, edited by A. Neimitz et al, Vol. I, pp. 13-19, 2002.
12. Abot, J.L., Daniel, I.M. and E.E. Gdoutos, Contact Law for Composite Sandwich Beams, *Journal of Sandwich Structures and Materials*, Vol. 4, pp.157-173, 2002.
13. Gdoutos, E.E., Daniel, I.M., Wang, K.-A., Compression Facing Wrinkling of Composite Sandwich Structures, *Mechanics of Materials*, Vol. 35, pp. 511-522, 2003.
14. Daniel, I.M., Gdoutos, E.E., Abot, J.L. and Wang, K.-A., Core Failure of Sandwich Beams," in *Recent Advances in Composite Materials*, edited by E.E. Gdoutos and Z.P. Marioli-Riga, Kluwer Academic Publishers, pp. 279-290, 2003.
15. Daniel, I.M., Gdoutos, E.E. and Abot, J.L., Optical Methods for Analysis of Deformation and Failure of Composite Sandwich Beams, *Proceedings of the 2003 SEM Annual Conference*, June 2-4, 2003, Charlotte, North Carolina, 2003.

16. Hsiao, H. M., Daniel, I. M. and Wooh, S. C., A New Compression Test Method for Thick Composites, *Journal of Composite Materials*, Vol. 29, pp. 1789-1806, 1995.
17. Daniel, I. M. and Abot, J. L., Fabrication, Testing and Analysis of Composite Sandwich Beams, *Composites Science and Technology*, Vol. 60, No. 12-13, pp.2455-2463, 2000.
18. Gdoutos, E. E., Daniel, I. M. and Wang, K.-A., Failure of Cellular Foams under Multiaxial Loading, *Composites, Part A*, Vol. 33, pp. 163-176, 2002.
19. Heath, W. G., *Sandwich Construction, Part 2: The Optimum Design of Flat Sandwich Panels*, *Aircraft Engineering*, Vol. 32, pp. 230-235, 1969.
20. Vinson, J. R., *The Behavior of Sandwich Structures of Isotropic and Composite Materials*, Technomic Publishing Co., Lancaster, PA, USA (1999).
21. Gdoutos, E. E., Daniel, I. M. and Wang, K.-A., Indentation Failure in Composite Sandwich Structures, *Proc. 2001 SEM Annual Conf.*, June 4-6, 2001, Portland, Oregon, USA, pp.528-531, 2001.
22. Hoff, N. J. and Mautner, S. E., The Buckling of Sandwich-Type Panels, *Journal of Aerospace Sciences*, Vol. 12, pp. 285-297, 1945.